Asian Journal of Agriculture and Biology
https://doi.org/10.35495/ajab.2024.248

Original Article

In silico identification and characterization of potent laccase inhibitors against *Cryptococcus neoformans*: A multi-scale computational study

Muharib Alruwaili[1*†], Sonia Younas [2,3†], Muhammad Umer Khan[4*], Hammad Saleem[5], Yasir Alruwaili[1,6], Abualgasim Elgaili Abdalla[1], Bi Bi Zainab Mazhari[7], Khalid Abosalif[1], Hasan Ejaz[1]

[1]Department of Clinical Laboratory Sciences, College of Applied Medical Sciences, Jouf University, Sakaka 72388, Saudi Arabia

[2]Centre for Immunology and Infection (C2i), Hong Kong Science and Technology Park, Hong Kong, SAR China

[3]HKU-Pasteur Research Pole, School of Public Health, LKS Faculty of Medicine, The University of Hong Kong, Hong Kong, China

[4]Institute of Molecular Biology and Biotechnology, The University of Lahore, Lahore, 54590, Pakistan

[5]Institute of Pharmaceutical Sciences (IPS), University of Veterinary & Animal Sciences (UVAS), Lahore, Pakistan

[6]Sustainable Development Research and Innovation Center, Deanship of Graduate Studies and Scientific Research, Jouf University, Sakaka 72388, Saudi Arabia

[7]Department of Clinical Laboratory Sciences, College of Applied Medical Sciences, Jouf University, Qurayyat 75911, Saudi Arabia

[†] *These authors contributed equally*

**Corresponding authors' emails:* mfalrwaili@ju.edu.sa; muhammad.umer4@mlt.uol.edu.pk

Received: 30 November 2024 / Accepted: 27 January 2025 / Published Online: 06 March 2025

Abstract

Cryptococcus neoformans is an opportunistic fungal pathogen, especially affecting individuals with weakened immune systems. Laccase enzymes are pivotal in its pathogenicity, making them promising targets for therapeutic intervention. This study aims to identify and characterize potent laccase inhibitors against *C. neoformans* using advanced in-silico analysis. The laccase protein (UniProt ID: Q55P57) was retrieved via AlphaFold and validated with ProCheck. Pharmacophore-based virtual screening (PBVS) identified 19 potential inhibitors, which were docked using CB-Dock2. The top six compound's pharmacokinetic properties were assessed using SwissADME, PKCSM, and StopTox. Bioactivity was predicted via SwissTargetPrediction. Density Functional Theory (DFT) calculations were conducted using Gauss view 5.0.8. The validated 3D structure of the target protein Q55P57 demonstrated high quality, with 86.5% of residues in favored regions. The molecular docking revealed that L-11 exhibited the highest binding affinity (-13.2 kcal/mol), forming crucial interactions within the active site. L-11 displayed favorable physicochemical properties, including high lipophilicity and good Caco2 permeability, positioning it as a strong candidate for therapeutic development. Toxicity predictions indicated non-toxicity for acute inhalation and oral exposure, while bioactivity analysis highlighted its broad target interactions. DFT analysis demonstrated L-11's enhanced reactivity due to its high dipole moment and low HOMO-LUMO energy gap. The identification of L-11 (8-[4-[9,9-Dimethyl-7-(2,3,4,5,6,7,8,9,10-nonahydroxypyren-1-yl)fluoren-2-yl]phenyl]pyrene-1,2,3,4,5,6,7,9,10-nonol) as a potent inhibitor of *C. neoformans* laccase represents a novel approach to antifungal drug discovery, marking a significant step to combat fungal infections and a way forward to perform in-vitro and in-vivo studies and ultimately its clinical application.

Keywords: *C. neoformans*, Ellagic acid, Laccase inhibitor, Molecular docking, ADMET, Antifungal

Graphical Abstract

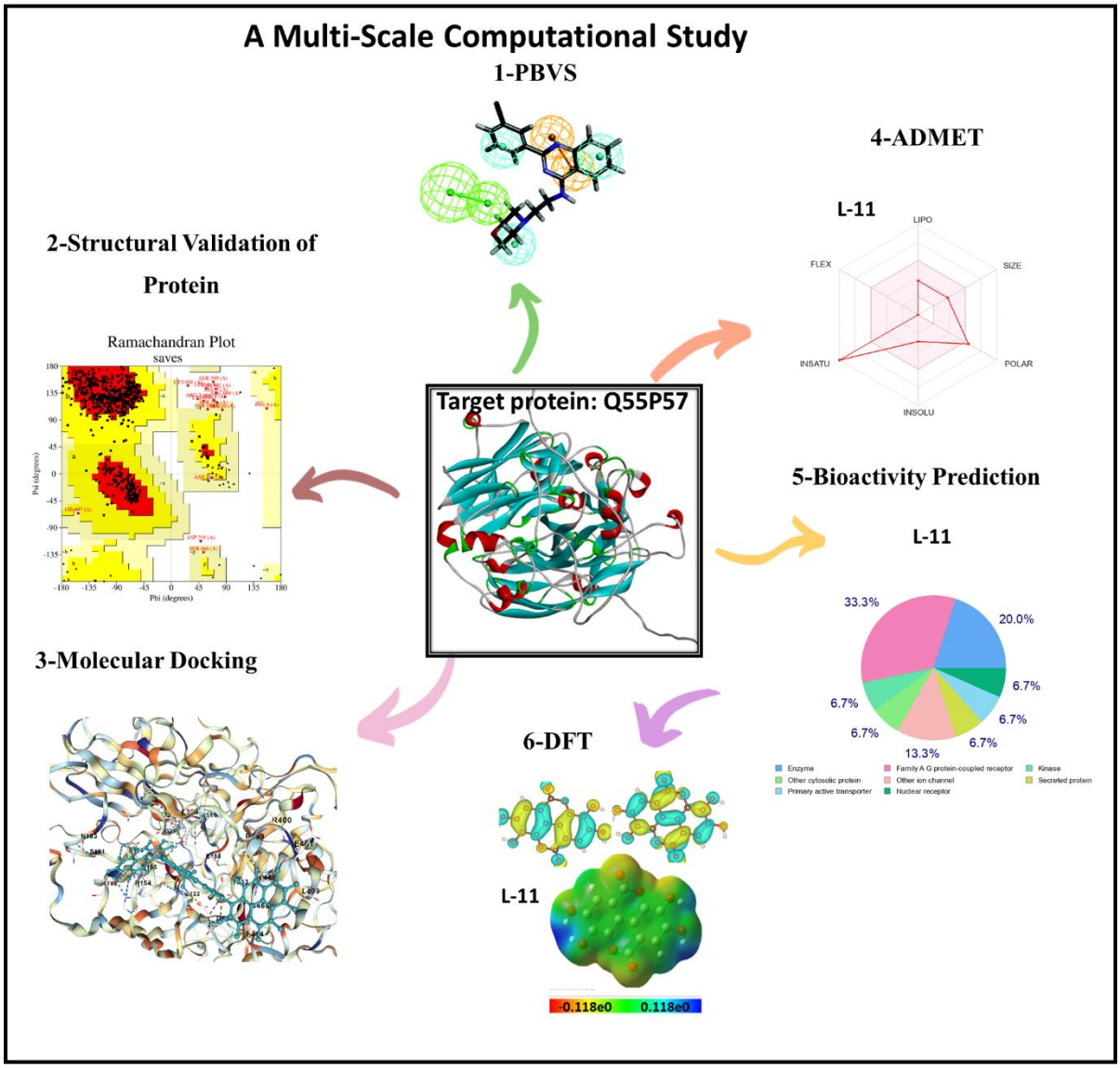

How to cite this article:
Alruwaili M, Younas S, Khan MU, Saleem H, Alruwaili Y, Abdalla AE, Mazhari BBZ, Abosalif K and Ejaz H. In silico identification and characterization of potent laccase inhibitors against *Cryptococcus neoformans*: A multi-scale computational study. Asian J. Agric. Biol. 2025: 2024248. DOI: https://doi.org/10.35495/ajab.2024.248

Introduction

Fungal infections, particularly those caused by the genus Cryptococcus, Candida, Aspergillus, and Pneumocystis, can result in mortality rates exceeding 50%, making them some of the deadliest pathogens affecting humans (Bastos et al., 2021; Fisher et al., 2022). *Cryptococcus neoformans (C. neoformans*) is the causative agent for most life-threatening systemic cryptococcosis cases. Infection with this pathogen accounts for prominent morbidity and mortality rates worldwide. In 2022, the WHO included *C. neoformans* in its leading fungal priority pathogen list (WHO, 2022). Cryptococcosis primarily affects the lungs or central nervous system (CNS), though in some cases, the disease can disseminate to other organs while still presenting localized symptoms (WHO, 2022). This condition frequently affects individuals with weakened immune systems especially those suffering from cancer, HIV, or patients receiving treatment for chemotherapy and organ transplant (Datta et al., 2016).

C. neoformans possesses several key virulence factors, including its ability to thrive at body temperature, produce a polysaccharide capsule, and synthesize laccase enzyme. This enzyme facilitates melanin production, protecting the pathogen from both antifungal therapies and the host immune responses, while also supporting adhesion, sporulation, and fruiting body development (Zhu et al., 2001; Azam et al., 2022). Therefore, targeting laccase inhibition, either alone or in conjugation with other antifungal agents, could serve as viable approach to cryptococcal infections (Zhu et al., 2001). *C. neoformans* exhibits natural resistance to treatments like caspofungin, an agent that disrupt the synthesis of fungal cell wall (Mourad and Perfect, 2018; Qadri et al., 2021; Moreira-Walsh et al., 2022). Consequently, the standard treatment for cryptococcal infections often involves a combination of amphotericin B (AmB) and flucytosine (FC) (Mourad and Perfect, 2018). With the use of extended therapy, resistant cryptococcal strains can emerge, and toxicity related to the drugs may occur (Laniado-Laborín and Cabrales-Vargas, 2009).

The rise in a number of immunocompromised individuals has led to increased fungal infections, including those from *C. neoformans*, highlighting the urgent need for newer, more effective, and less toxic antifungal agents (Singh et al., 2015; Gutierrez-Gongora and Geddes-McAlister, 2022; Khan et al., 2024). The ineffectiveness of echinocandins, a novel category against *C. neoformans* presents a major obstacle, necessitating the development of novel antifungal medications with mechanisms distinct from traditional drugs (Huang et al., 2019). Recently, plant-derived compounds have been documented as showing promising potential for use in the treatment of various infectious diseases (Langeveld et al., 2014; Ayaz et al., 2019). Recent studies highlight ellagic acid (EA), a secondary metabolite and dietary polyphenol found in various plants including pomegranate, strawberry, raspberry, and cranberry, as a promising agent against *C. neoformans* (Sarkar et al., 2015). EA has therapeutic potential against a wide range of illnesses such as diabetes, oxidative stress, inflammatory conditions, hypertension, heart disorders, and increased cholesterol levels. It has also proved potentially effective for skin, liver, Alzheimer, Parkinson diseases, and cancer. Moreover, EA revealed antimicrobial activity against a wide range of infections (Ríos et al., 2018). One study of mice found a 70% survival rate after treatment with EA compared to only 20% treated with fluconazole (Khan et al., 2021). EA's ability to inhibit laccase activity was also proved by in-silico and in-vivo analysis (Azam et al., 2022).

The current study fills a major research gap in the management of *C. neoformans* infections by concentrating on the growing problem of drug resistance and the limited effectiveness of current antifungal treatments. The current research focuses on utilizing the most advanced in-silico approaches to identify and characterize potent inhibitors of laccase, a key enzyme critical to the virulence of *C. neoformans.* By targeting laccase, the research seeks to address the pressing need for novel antifungal therapies. The study focuses on leveraging computational methods, including pharmacophore-based virtual screening, molecular docking, pharmacokinetic, and toxicity analysis. DFT analysis, to evaluate the potential inhibitors, with specific emphasis on plant-derived compounds. Through these computational analyses, the research aims to provide a foundation for developing antifungal strategies and facilitates the transition from computational predictions to in-vitro, in-vivo, and eventually clinical applications.

https://doi.org/10.35495/ajab.2024.248

Material and Methods

Target protein retrieval and structure validation

The laccase protein from *C. neoformans*, which is encoded by the laccase 1(LAC1) gene, was identified using UniProt database (UniProt ID: Q55P57) (https://www.uniprot.org/). Since no experimental structure was available in PDB, a conformation of this protein was downloaded from AlphaFold (https://alphafold.ebi.ac.uk/). AlphaFold was chosen due to its proven ability to accurately predict the protein structures with high confidence, particularly in cases where experimental data is lacking (Varadi et al., 2024). The protein consists of a single A chain comprising 624 amino acid residues.

Structure validation

For the structure validation of the Q55P57 protein, the SAVES v6.0 (saves.mbi.ucla.edu/) server was used to ensure model quality and accuracy. Initially, the model was subjected to ERRAT analysis, which evaluated the overall quality factor based on non-bonded atomic interactions identifying potential errors in the protein model (Colovos and Yeates, 1993). The Ramachandran plot generated by ProCheck provided a detailed evaluation of phi (Φ) and psi (Ψ) angles for stereochemical quality (Laskowski et al., 1996).

Pharmacophore-based virtual screening (PBVS)

PBVS was carried out through the Pharmit database to find potential *C. neoformans* inhibitors. Based on the known features of the reference molecule, EA as a laccase inhibitor, a pharmacophore model was developed. The Pharmit database (https://pharmit.csb.pitt.edu/) was used to find a similar compound matching by using this developed pharmacophore model (Sunseri and Koes, 2016). The top 19 compounds from this search were chosen based on high RMSD scores.

Molecular docking studies

Virtual screening resulted in the identification of 19 hits, which included compounds against the selected target of *C.* neoformans, and were then analyzed via molecular docking with CB-Dock2 server, using AutoDock Vina v. 1.2.0, with an emphasis on structure-based blind docking (Liu et al., 2022; Khan et al., 2024). ChemDraw Professional, version 16.0 was used to design the 2D and 3D structures of the compounds (Norhayati et al., 2023). The protein's structure was submitted in PDB format, whereas the ligand was provided in SDF format. Both these formats were reprocessed by the CB-Dock2 server to prepare for docking (Sakhawat et al., 2024). The initial 3D conformation of the ligand was generated using RDKit, with hydrogens and partial charges automatically added by the server. The protein was checked for missing side chains and hydrogen atoms, and flagged for any missing residues (Cao et al., 2011). Co-crystallized water molecules and other heteroatoms were removed to create an accurate docking environment. Once submitted, CB-Dock2 automatically detects the cavity based on a curvature-based detection method (Yang et al., 2022). It predicts where the binding pocket on that protein is, interacting with the ligand (Sakhawat et al., 2023). Once the cavities have been identified, molecular docking with the aid of AutoDock Vina was conducted (Eberhardt et al., 2021). The tool undertakes a blind docking manner in which the ligand is automatically placed in the calculated cavities, searching various binding modes. The docking results include ligand binding poses in selected cavities and their binding affinity scores were used to analyze the best binding orientation and interaction strength between the ligand and protein.

Evaluation of pharmacokinetic properties

The pharmacokinetic properties including absorption, distribution, metabolism, and excretion were analyzed using PKCSM server (biosig.lab.uq.edu.au/pkcsm/). The SMILES were provided as input and results were visualized to compare the pharmacokinetic profiles. This analysis aims to identify compounds with favorable ADME characteristics as drug candidates, which are critical for their potential in vivo efficacy and bioavailability (Pires et al., 2015).

Toxicity prediction

Toxicity prediction was performed via the StopTox (stoptox.mml.unc.edu/) platform, which employs QSAR models to assess systemic and topical toxicity. After inputting the SMILES strings of the selected compounds in the tool, it predicts toxicological endpoints such as acute oral, dermal, and inhalation toxicity, and skin sensitization, irritation, and corrosion. This step is essential for identifying potentially hazardous compounds early in the drug

discovery pipeline, ensuring the selection of safer candidates for further in vivo testing. This approach offers a non-animal alternative for testing chemical safety in the process of drug discovery (Borba et al., 2022; Islam et al., 2024).

Bioactivity evaluation

The Swiss Target Prediction (SwissTargetPrediction) is employed in the prediction of ligand-based target. This method set forth the most likely protein targets for which the bioactive molecule exhibited high scores based on the provided SMILES strings of the query molecules (Daina and Zoete, 2024).

DFT calculations

The selected compounds were designed in 3D geometries using GaussView, version 5.0.8, and optimized with the Gaussian 09W program. The B3LYP/6-31G (d) methodology was used for both optimization and frequency calculations in the CPCM phases. To evaluate quantum chemical parameters, calculations were performed including HOMO and LUMO energy levels, along with the energy band gap (ΔE_{Gap}). Furthermore, molecular electrostatic potential (MEP) analysis was conducted using the DFT approach to explore the physicochemical properties of the compounds. Additionally, the DFT method was employed to conduct molecular electrostatic potential (MEP) analysis, aiming to investigate the physiochemical characteristics (Orio et al., 2009).

Results

Retrieval of target protein and structure validation

The 3D structure of the target protein with UniProt ID: Q55P57 was obtained from AlphaFold and visualized using discovery studio as shown in Figure 1. The protein contains single chain with 624 amino acid and exhibits well-defined secondary structural elements, including alpha-helices (red), beta-sheets (cyan), and loops (grey), shown through a color-coded visualization. The structure's overall folding displays a compact core with extended loop regions, which may be important for its biological activity, particularly in protein interactions or binding.

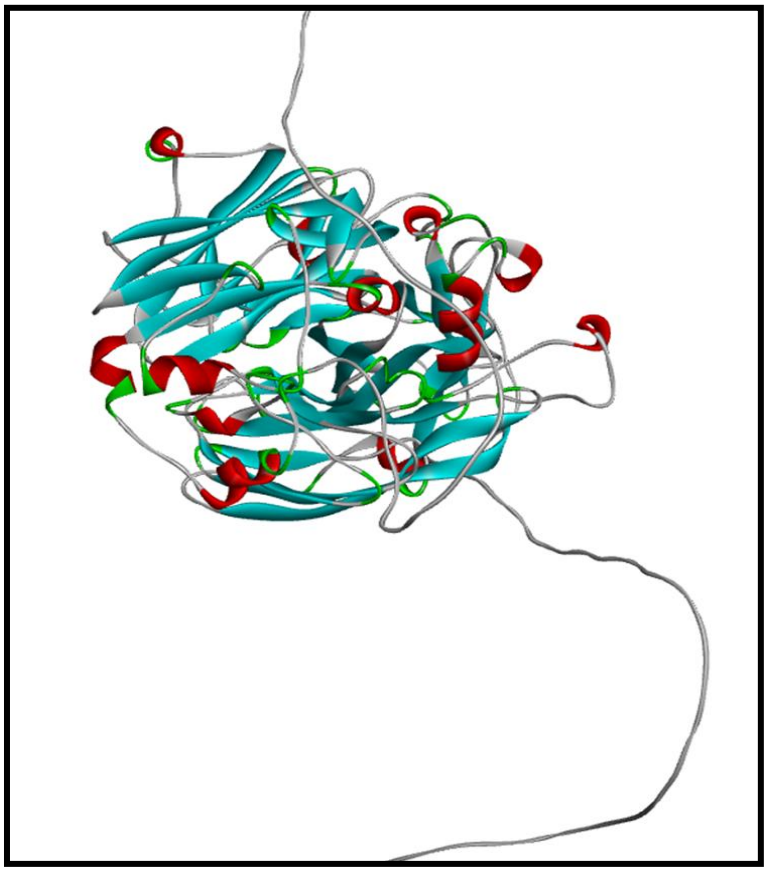

Figure-1: 3D Structure of the Target Protein (UniProt ID=Q55P57)

https://doi.org/10.35495/ajab.2024.248

Structure validation

The ERRAT analysis for the laccase protein (UniProt ID: Q55P57) showed an overall quality factor of 88.56%, which indicated a high-quality structure as shown in Figure 2. The error value graph indicates regions with different error rates. Most of the residues are below the acceptable thresholds for error (95% and 99%), indicating reliable structural integrity. However, certain residues, in particular around positions 180–200 and 480–500, have very high error values above the 99% threshold, pointing to potential structural inaccuracies or regions that need refinement. These observations suggested that while the overall model is robust, targeted corrections in these high-error regions may enhance the structure's reliability.

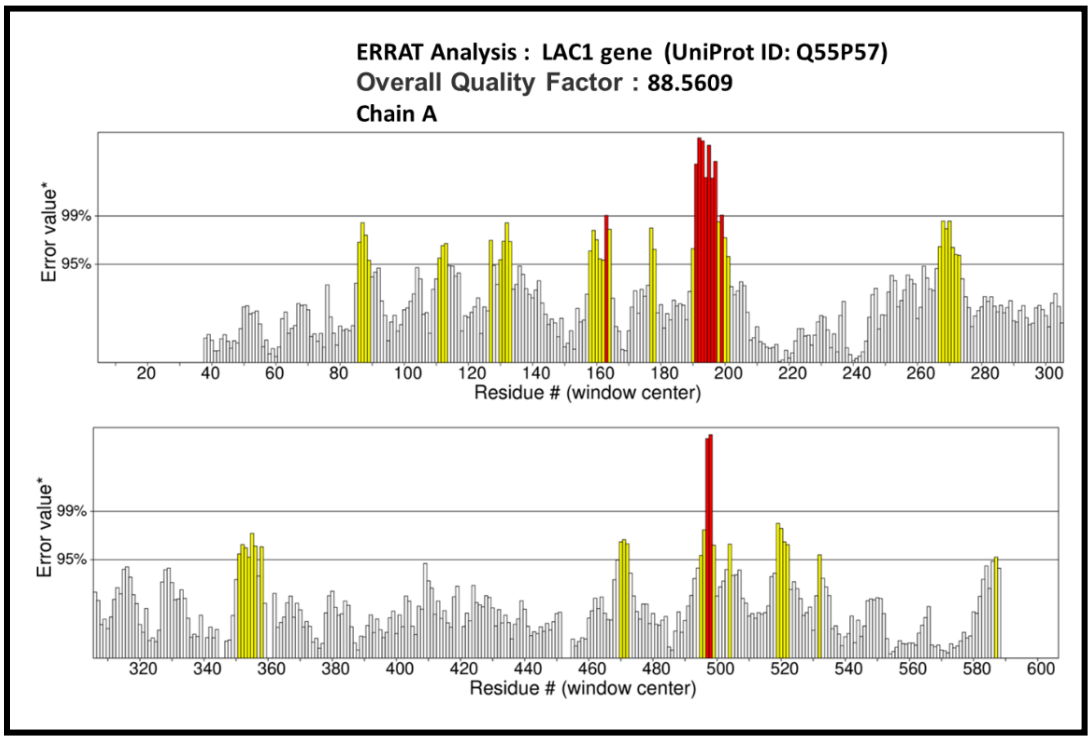

Figure-2: ERRAT2 Analysis of Structural Quality of Target Protein (UniProt ID: Q07973).

The Ramachandran plot (Figure 3), generated using the Procheck tool, was utilized to further validate and assess the structural integrity of the protein. The plot indicated that 86.5% of the residues lie within the highly favored regions, 10.2% in allowed regions, and only 1.9% in disallowed regions, indicating minimal structural anomalies. This analysis confirms that the protein adopts energetically favorable conformations, with most φ (phi) and ψ (psi) backbone dihedral angles falling within acceptable ranges. Such validation ensures that the structure is of high quality, supporting its reliability for further computational studies and functional analyses.

https://doi.org/10.35495/ajab.2024.248

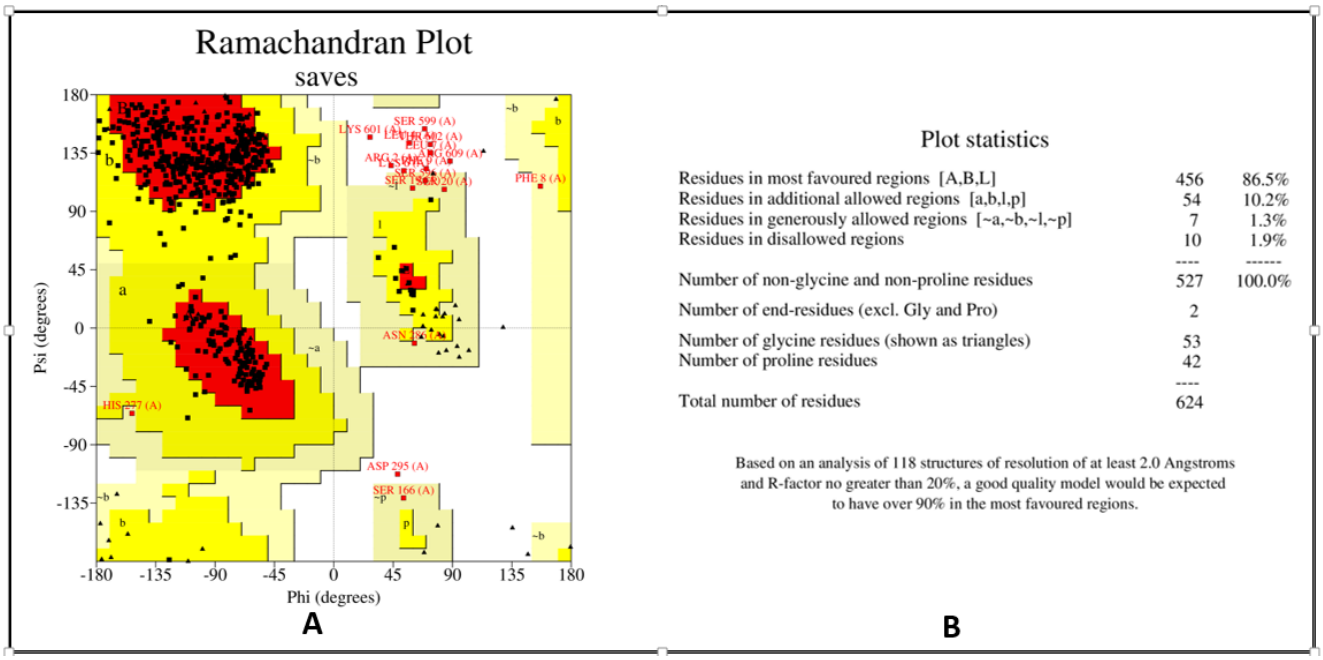

Figure-3: Structural Validation of Protein Q55P57 by Procheck Ramachandran Plot

Virtual screening

The Pharmit database was used to conduct PBVS. The 3D structure of the LAC1 enzyme from *C. neoformans* (UniProt ID: Q55P57), was used as the target for identifying potential inhibitors. Compounds were identified based on their alignment with a pharmacophore model derived from EA, a known LAC 1 inhibitor. From this screening, 19 compounds with high docking scores, indicating strong similarity to the pharmacophore model, were selected for further computational analysis, as detailed in Table 1.

Table-1: 2D and 3D Structures with SMILES of the Top 19 Compounds Selected by PBVS.

Code	Names	2D	3D	SMILES
L-1	Ellagic acid	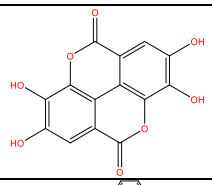	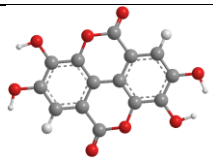	C1=C2C3=C(C(=C1O)O)OC(=O)C4=CC(=C(C(=C43)OC2=O)O)O
L-2	7-[10-(4-Phenylphenyl)anthracen-9-yl]naphthalene-1,2,3,4,5,6,8-heptol	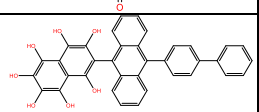	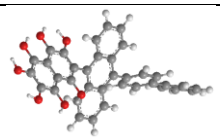	C1=CC=C(C=C1)C2=CC=C(C=C2)C3=C4C=CC=CC4=C(C5=CC=CC=C53)C6=C(C7=C(C(=C6O)O)C(=C(C(=C7O)O)O)O)O
L-3	9-(2,3,4,5,6,7,8-Heptahydroxynaphthalen-1-yl)-10-(4-naphthalen-2-ylphenyl)anthracene-1,2,3,4,5,6,7-heptol	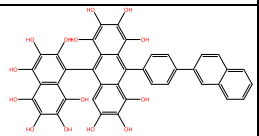	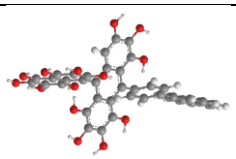	C1=CC=C2C=C(C=CC2=C1)C3=CC=C(C=C3)C4=C5C(=C(C6=CC(=C(C(=C64)O)O)O)O)C7=C(C(=C(C8=C7C(=C(C(=C8O)O)O)O)O)O)O)C(=C(C(=C5O)O)O)O

L-4	7-[4-[4-(1,3,4,5,6,7,8-heptahydroxynaphthalen-2-yl)-2,3,5,6-tetrahydroxyphenyl]-2,5,6,7,8-pentahydroxy-3-[(1Z)-1,2,3-trihydroxybuta-1,3-dienyl]naphthalen-1-yl]naphthalene-1,2,3,4,5,6,8-heptol	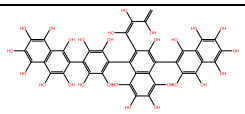	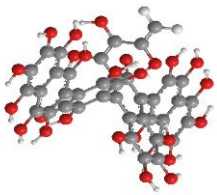	C=C(/C(=C(\C1=C(C2=C(C(=C1O)C3=C(C4=C(C(=C3O)O)C(=C(C(=C4O)O)O)O)O)C(=C(C(=C2O)O)O)O)C5=C(C(=C(C(=C5O)O)C6=C(C7=C(C(=C6O)O)C(=C(C(=C7O)O)O)O)O)O)O)/O)/O)O
L-5	9-(4-Dibenzofuran-2-ylphenyl)-7,10-bis(2,3,4,5,6,7,8-heptahydroxynaphthalen-1-yl)anthracene-1,2,3,4,5,6,8-heptol	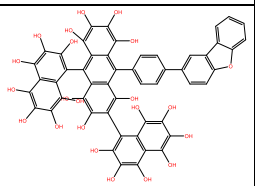	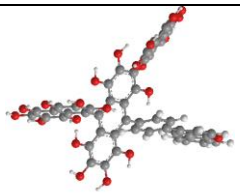	C1=CC=C2C(=C1)C3=C(O2)C=CC(=C3)C4=CC=C(C=C4)C5=C6C(=C(C7=C5C(=C(C(=C7O)O)C8=C(C(=C(C9=C8C(=C(C(=C9O)O)O)O)O)O)O)O)C1=C(C(=C(C2=C1C(=C(C(=C2O)O)O)O)O)O)O)C(=C(C(=C6O)O)O)O
L-6	7-[10-(2,3,6-Trihydroxy-4,5-diphenylphenyl)anthracen-9-yl]naphtho[5,6-b][1]benzofuran-1,2,3,4,5,6,8,9,10-nonol	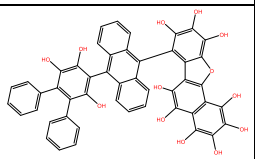	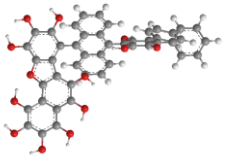	C1=CC=C(C=C1)C2=C(C(=C(C(=C2O)C3=C4C=CC=CC4=C(C5=CC=CC=C53)C6=C7C8=C(C9=C(C(=C8O)O)C(=C(C(=C9O)O)O)O)O)OC7=C(C(=C6O)O)O)O)O)C1=CC=CC=C1
L-7	9,10-bis(2,3,4,5,6,7,8-heptahydroxynaphthalen-1-yl)-7-[(3Z)-3-(4,5,6,7,8,9-hexahydroxy-1-methylidenebenzo[e][1]benzofuran-2-ylidene)-1,1,3-trihydroxyprop-1-en-2-yl]anthracene-1,2,3,4,5,6,8-heptol	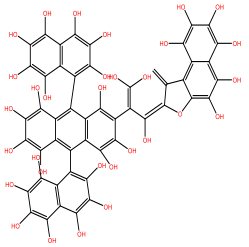	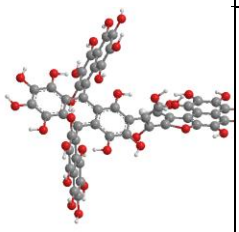	C=C\1C2=C3C(=C(C(=C2O/C1=C(/C(=C(O)O)C4=C(C5=C(C(=C6C(=C5C7=C(C(=C(C8=C7C(=C(C(=C8O)O)O)O)O)O)O)O)C(=C(C(=C6O)O)O)O)C9=C(C(=C(C1=C9C(=C(C(=C1O)O)O)O)O)O)O)C(=C4O)O)O)\O)O)O)C(=C(C(=C3O)O)O)O
L-8	9-(1,3,4,5,6,7,8-Heptahydroxynaphthalen-2-yl)-10-[2,3,4,5-tetrahydroxy-6-(2,3,4,5,6-pentahydroxyphenyl)phenyl]anthracene-1,2,3,4,5,6,7,8-octol	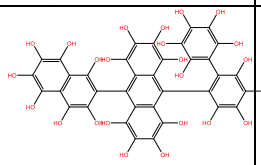	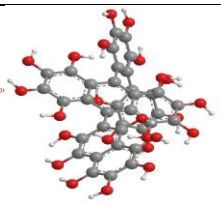	C1(=C2C(=C(C3=C1C(=C(C(=C3O)O)O)O)O)C4=C(C5=C(C(=C4O)O)C(=C(C(=C5O)O)O)O)O)C(=C(C(=C2O)O)O)O)C6=C(C(=C(C(=C6O)O)O)O)O)C7=C(C(=C(C(=C7O)O)O)O)O
L-9	1-[10-(2,3,4,5,6,7,8-Heptahydroxynaphthalen-1-yl)-1,2,3,4,5,6,7,8-octahydroxyanthracen-9-yl]naphtho[6,7-b][1]benzofuran-2,3,4,6,7,8,9,10,11-nonol	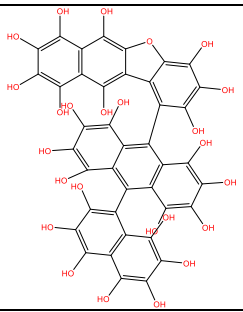	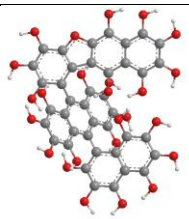	C1(=C2C(=C(C3=C1C(=C(C(=C3O)O)O)O)O)C4=C(C(=C(C5=C4C(=C(C(=C5O)O)O)O)O)O)O)O)C(=C(C(=C2O)O)O)O)C6=C7C8=C(C9=C(C(=C(C(=C9O)O)O)O)O)C(=C8OC7=C(C(=C6O)O)O)O)O
L-10	9-Hydroxycarbazole-1,2,3,4,5,6,7,8-octol	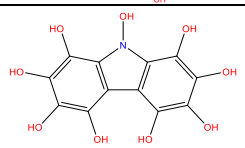	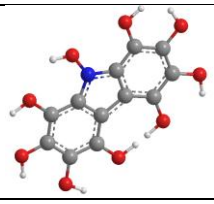	C12=C(C(=C(C(=C1O)O)O)O)N(C3=C2C(=C(C(=C3O)O)O)O)O

L-11	8-[4-[9,9-Dimethyl-7-(2,3,4,5,6,7,8,9,10-nonahydroxypyren-1-yl)fluoren-2-yl]phenyl]pyrene-1,2,3,4,5,6,7,9,10-nonol	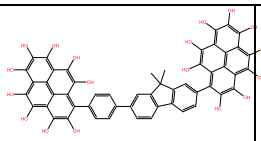	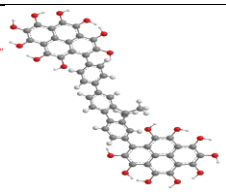	CC1(C2=C(C=CC(=C2)C3=CC=C(C=C3)C4=C5C6=C7C(=C(C(=C6C(=C4O)O)O)O)C(=C(C(=C7C(=C5O)O)O)O)O)C8=C1C=C(C=C8)C9=C1C2=C3C(=C(C(=C2C(=C9O)O)O)O)C(=C(C(=C3C(=C1O)O)O)O)O)C
L-12	Naphthalene-1,2,3,7,8-pentol	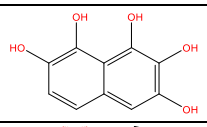	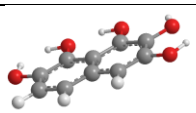	C1=CC(=C(C2=C(C(=C(C=C21)O)O)O)O)O
L-13	9-[10-(1,3,4,5,6,7,8-Heptahydroxynaphthalen-2-yl)anthracen-9-yl]naphtho[5,6-b][1]benzofuran-1,2,3,4,5,6,7,8,10-nonol	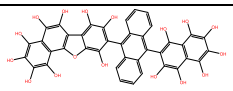	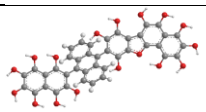	C1=CC=C2C(=C1)C(=C3C=CC=CC3=C2C4=C(C(=C5C6=C(C7=C(C(=C6O)O)C(=C(C(=C7O)O)O)O)OC5=C4O)O)O)C8=C(C9=C(C(=C8O)O)C(=C(C(=C9O)O)O)O)O
L-14	10-[4-(2,3,4,5,6,7,8-Heptahydroxynaphthalen-1-yl)-2,3,5,6-tetrahydroxyphenyl]anthracene-1,2,3,4,5,6,7,8,9-nonol	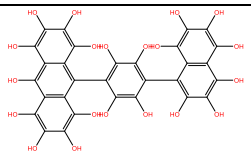	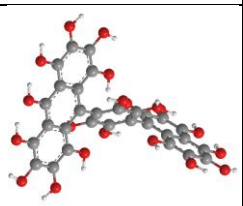	C1(=C2C(=C(C3=C1C(=C(C(=C3O)O)O)O)O)C(=C(C(=C2O)O)O)O)C4=C(C(=C(C(=C4O)O)C5=C(C(=C(C6=C5C(=C(C(=C6O)O)O)O)O)O)O)O)O
L-15	3,6-Bis[4-(2,3,4,5,6,7,8-heptahydroxynaphthalen-1-yl)-2,3,5,6-tetrahydroxyphenyl]pyrene-1,2,4,5,7,8,9,10-octol	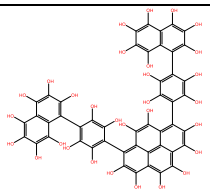	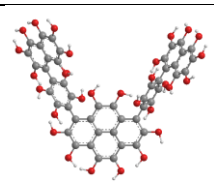	C12=C3C4=C(C(=C(C3=C(C(=C1C(=C(C(=C2C(=C4O)O)C5=C(C(=C(C(=C5O)O)C6=C(C(=C(C7=C6C(=C(C(=C7O)O)O)O)O)O)O)O)O)O)O)O)O)O)C8=C(C(=C(C(=C8O)O)C9=C(C(=C(C1=C9C(=C(C(=C1O)O)O)O)O)O)O)O)O)O
L-16	Naphthalene-1,2,3,4,5,6,7-heptol	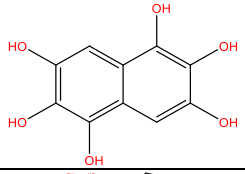	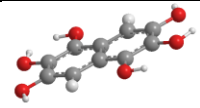	C1=C2C(=C(C(=C1O)O)O)C(=C(C(=C2O)O)O)O
L-17	9-[10-(4-Cyclohexa-2,4-dien-1-ylnaphthalen-2-yl)-3,4-dihydroanthracen-9-yl]naphtho[5,6-b][1]benzofuran-1,2,3,4,5,6,7,8,10-nonol	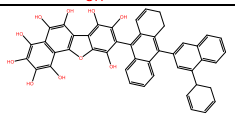	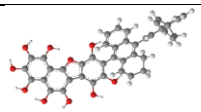	C1CC2=C(C3=CC=CC=C3C(=C2C=C1)C4=C(C(=C5C6=C(C7=C(C(=C6O)O)C(=C(C(=C7O)O)O)O)O)OC5=C4O)O)O)C8=CC9=CC=CC=C9C(=C8)C1CC=CC=C1
L-18	9-Dibenzofuran-1-yl-10-(2,3,4,5,6,7-hexahydroxynaphthalen-1-yl)anthracene-1,2,3,4,5,6,7,8-octol	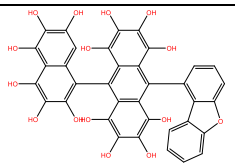	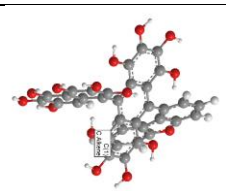	C1=CC=C2C(=C1)C3=C(C=CC=C3O2)C4=C5C(=C(C6=C4C(=C(C(=C6O)O)O)O)O)C7=C(C(=C(C8=C(C(=C(C=C78)O)O)O)O)O)O)C(=C(C(=C5O)O)O)O
L-19	8-[4-(8-Dibenzofuran-4-ylpyren-1-yl)-2,3,5,6-tetrahydroxyphenyl]naphthalene-1,2,3,4,5,6-hexol	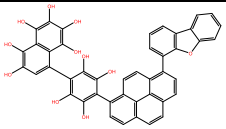	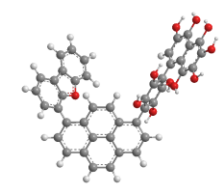	C1=CC=C2C(=C1)C3=C(O2)C(=CC=C3)C4=C5C=CC6=C(C=CC7=C6C5=C(C=C7)C=C4)C8=C(C(=C(C(=C8O)O)C9=CC(=C(C1=C9C(=C(C(=C1O)O)O)O)O)O)O)O)O

Molecular docking analysis

All the 19 shortlisted compounds underwent molecular docking analysis, among them the top six, including the reference molecule EA, were selected for further analysis against the LAC1 enzyme of *C. neoformans* based on their high docking score. The selection of these compounds was based on their docking scores, as outlined in Table 2. The reference compound, Ellagic acid (L-1), has indicated good binding affinity (-8.0 kcal/mol). In contrast, the top five compounds demonstrated significantly stronger interactions, with L-11 scoring -13.2 kcal/mol the highest among them suggesting it binds very strongly to the target enzyme. L-5 follows closely with -12.8 kcal/mol, while L-17, L-15, and L-3 show scores of -12.3, -12.1, and -11.7 kcal/mol, respectively. These results indicate that these compounds, mainly the L-11 has considerable potential as effective inhibitors of the LAC1 enzyme against *C. neoformans* infections, warranting further investigation.

Table-2: Docking score of top-hit compounds.

Code	Names	Docking Score (kcal/mol)
L-1 (Reference Compound)	Ellagic acid (Reference Compound)	-8.0
L-11	8-[4-[9,9-Dimethyl-7-(2,3,4,5,6,7,8,9,10-nonahydroxypyren-1-yl)fluoren-2-yl]phenyl]pyrene-1,2,3,4,5,6,7,9,10-nonol	-13.2
L-5	9-(4-Dibenzofuran-2-ylphenyl)-7,10-bis(2,3,4,5,6,7,8-heptahydroxynaphthalen-1-yl)anthracene-1,2,3,4,5,6,8-heptol	-12.8
L-17	9-[10-(4-Cyclohexa-2,4-dien-1-ylnaphthalen-2-yl)-3,4-dihydroanthracen-9-yl]naphtho[5,6-b][1]benzofuran-1,2,3,4,5,6,7,8,10-nonol	-12.3
L-15	3,6-Bis[4-(2,3,4,5,6,7,8-heptahydroxynaphthalen-1-yl)-2,3,5,6-tetrahydroxyphenyl]pyrene-1,2,4,5,7,8,9,10-octol	-12.1
L-3	9-(2,3,4,5,6,7,8-Heptahydroxynaphthalen-1-yl)-10-(4-naphthalen-2-ylphenyl)anthracene-1,2,3,4,5,6,7-heptol	-11.7

Docking of the reference compound EA (L-1) with *C. neoformans* LAC1 (Q55P57) is shown in Figure 4, illustrating the ligand's interaction within the enzyme's binding pocket. EA (L-1) interacts by binding to its active site, where it forms crucial interactions with amino acid residues such as His154, Ser156, Tyr159, Arg516, and others. These interactions, primarily through hydrogen bonding and non-covalent forces, stabilize EA within the binding pocket. The interaction with these amino acid residues is likely crucial for the compound’s potential to inhibit enzyme function.

https://doi.org/10.35495/ajab.2024.248

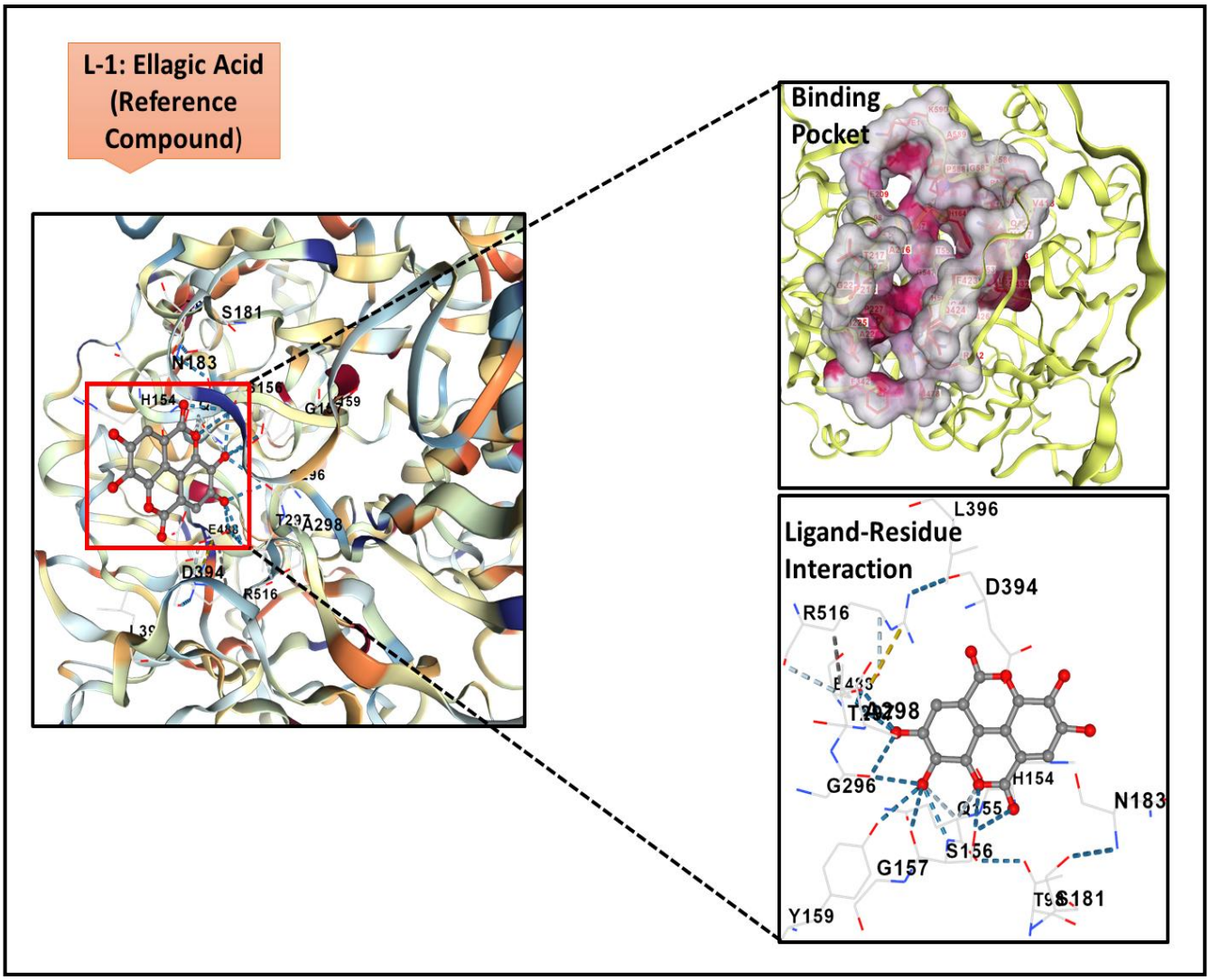

Figure-4: Molecular Docking of Ellagic Acid (L-1) with Target Protein (Q55P57) Showing Binding Pocket and Ligand-Residue Interactions.

The molecular docking results revealed that the top three ligands (L-11, L-5, and L-17) demonstrated strong interactions with the active site of *C. neoformans* LAC1 (Protein ID: Q55P57) as shown in Figure 5. L-11, which fits deeply into the active site, forms a robust network of interactions, including hydrogen bonds with residues such as H154, S166, T297, and D394, as well as hydrophobic contacts with L396 and F454. These interactions likely contribute to its high binding affinity. Similarly, L-5 exhibited favorable interactions, primarily through hydrogen bonds with residues N421, V418, and T422, further supporting its potential inhibitory effect. Significant engagement between L-17 and residues Y433, Q434, and S432 indicated crucial binding pocket interactions. Strong binding affinities of these ligands were demonstrated by the hydrogen bonds and other stabilizing interactions found in these complexes, which offered important information on their potential as laccase inhibitors against *C. neoformans.*

https://doi.org/10.35495/ajab.2024.248

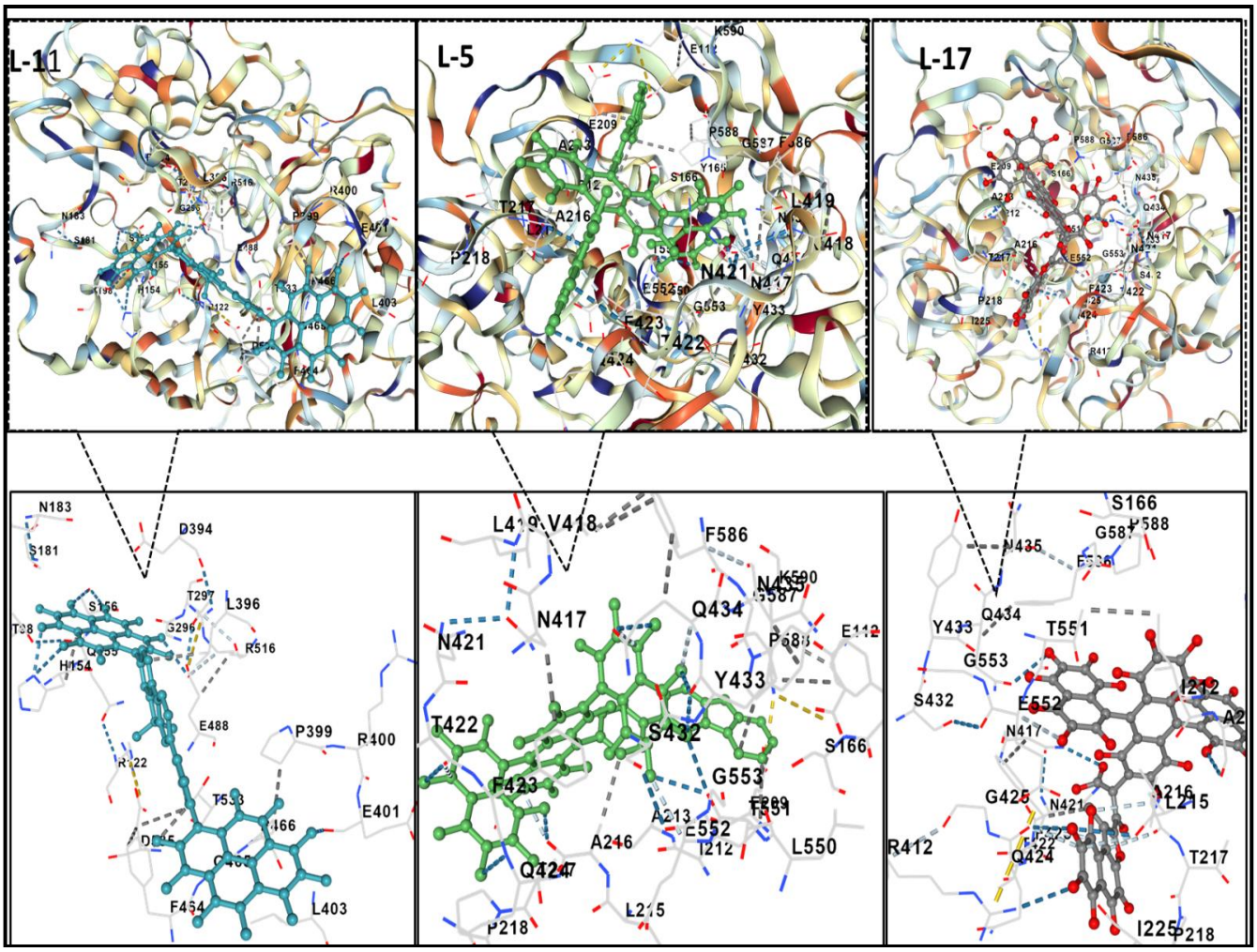

Figure-5: Molecular Docking Interactions of Top Three Ligands (L-11, L-5, L-17) with Target Protein Q55P57

The detailed molecular docking analysis of ligands L-15 and L-3 with the target protein Q55P57 is summarized in Figure 6. L-15 interacts with three important residues S156, H154, and R122 via hydrogen interactions which show strong stabilizing forces to support its high binding specificity. Moreover, other active site residues also affected L-15 positioning and identification of its binding to the enzyme; this made L-15 highly stable within the binding pockets. L-3 also displayed good hydrogen bond contacts especially with N421, F423, and Y433 providing additional evidence of its tight binding in the active site. The hydrogen bonds and other stabilizing interactions identified for both ligands highlighted their potential efficacy as inhibitors, suggesting their suitability for further investigation as therapeutic candidates.

https://doi.org/10.35495/ajab.2024.248

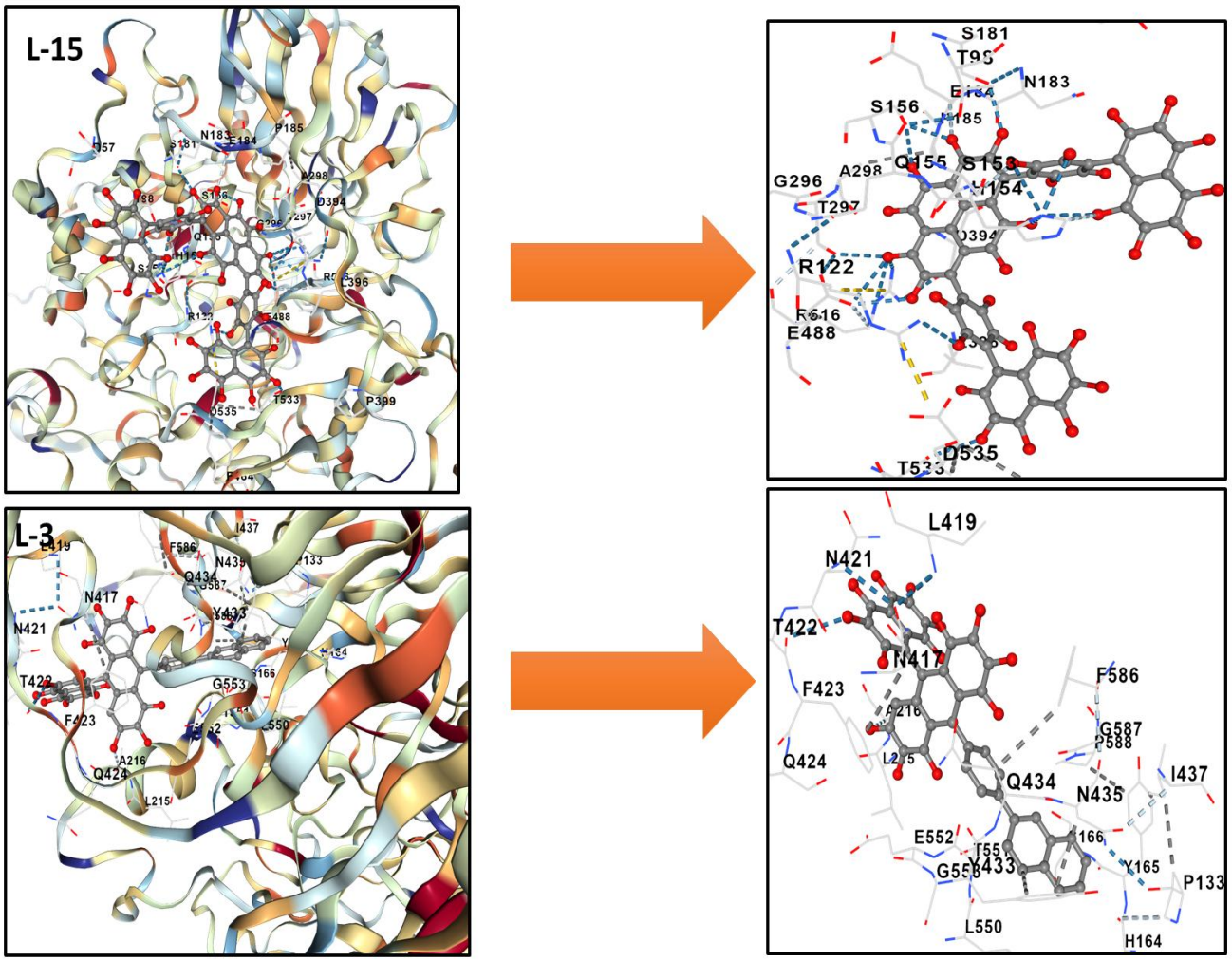

Figure-6: Molecular Docking Interactions of L-15 and L-3 with Target Protein Q55P57

Pharmacokinetic properties assessment

The pharmacokinetic characteristics of the selected compounds (L-1, L-11, L-5, L-17, L-15, and L-3) based on their high docking scores provide an understanding of their absorption, distribution, metabolism, excretion, and toxicity, which are essential for evaluating their therapeutic potential as detailed in Table 3.

Pharmacokinetic properties such as absorption and skin permeability determine the bioavailability and effective delivery of these compounds to target sites, including the potential to penetrate fungal biofilms or interact with skin surfaces for topical applications. In terms of absorption, all compounds exhibited low water solubility, with L-1 being the least soluble and L-11 showing moderate solubility. L-11 demonstrated better Caco2 permeability indicating good potential absorption in the human intestines. Skin permeability analysis revealed L-11 to have favorable transdermal delivery potential, which is critical for compounds intended for topical antifungal treatments. L-17 has the highest predicted intestinal absorption at 100%.

Regarding distribution, L-11 has a relatively higher volume of distribution, and a higher fraction of unbound remains free in the bloodstream, indicating good tissue distribution and availability for pharmacological activity. Most compounds are CYP3A4 substrates, suggesting they may undergo hepatic metabolism, and L-15 is identified as a CYP3A4 inhibitor, which could lead to drug interactions. In terms of excretion, L-1 exhibited positive total clearance, indicating efficient

elimination, whereas L-11 showed reduced clearance. Effective excretion is favorable for minimizing potential accumulation and toxicity during prolonged treatment. Toxicity profiles revealed that L-1 may be potentially mutagenic, while L-11 appeared safer, with a moderate maximum tolerated dose and no hERG I inhibition, though it does show potential to inhibit hERG II. Overall, L-11 stands out due to its favorable absorption, moderate distribution, and acceptable safety profile, making it a promising candidate for therapeutic development against fungal infections, particularly against *C. neoformans*.

Table-3: Pharmacokinetic Parameters of the Selected Compounds Analyzed by pkCSM

Pharmacokinetic Properties		**Selected Compounds**					
Properties	**Model Name**	**L-1**	**L-11**	**L-5**	**L-17**	**L-15**	**L-3**
Absorption	**Water solubility** (log mol/L)	-3.362	-2.892	-2.892	-3.078	-2.892	-2.946
	Caco2 Permeability (log Papp in 10^{-6} cm/s)	-0.273	-0.955	-1.352	-0.198	-2.375	-0.793
	Intestinal Absorption (%)	80.032	59.538	35.891	100	0	-0.793
	Skin Permeability (Log Kp)	-3.376	-2.735	-2.735	-2.735	-2.735	-2.735
	P-glycoprotein Substrate (Yes/No)	Yes	Yes	Yes	Yes	Yes	Yes
	P-glycoprotein I Inhibitor (Yes/No)	No	Yes	Yes	Yes	Yes	Yes
	P-glycoprotein II Inhibitor (Yes/No)	No	Yes	Yes	Yes	Yes	Yes
Distribution	**VDss (human) (log L/Kg)**	-1.214	-0.368	-0.291	-0.775	-0.167	-0.953
	Fraction unbound (human) (Fu)	0.27	0.344	-0.359	0.132	0.372	0.224
	BBB Permeability (log BBB)	-1.054	-2.713	-3.389	-1.442	-4.934	-2.154
	CNS Permeability (log PS)	-3.144	-2.965	-3.506	-1.934	-5.423	-2.935
Metabolism	**CYP2D6 Substrate (Yes/No)**	No	No	No	No	No	No
	CYP3A4 Substrate (Yes/No)	Yes	Yes	Yes	Yes	Yes	Yes
	CYP1A2 Inhibitor (Yes/No)	Yes	No	No	No	No	No
	CYP2C19 Inhibitor (Yes/No)	No	No	No	No	No	No
	CYP2C9 Inhibitor (Yes/No)	No	No	No	No	No	No
	CYP2D6 Inhibitor (Yes/No)	No	No	No	No	No	No
	CYP3A4 Inhibitor (Yes/No)	No	No	No	No	Yes	No
Excretion	**Total Clearance (log ml/min/kg)**	0.539	-0.132	0.165	-0.072	-0.36	0.004
	Renal OCT2 substrate (Yes/No)	No	No	No	No	No	No
Toxicity	**AMES toxicity (Yes/No)**	Yes	No	No	No	No	No
	Max. tolerated dose (human) (log mg/kg/day)	0.777	0.417	0.429	0.329	0.437	0.362
	hERG I inhibitor (Yes/No)	No	No	No	No	No	No
	hERG II inhibitor (Yes/No)	No	Yes	Yes	Yes	Yes	Yes
	Oral Rat Acute Toxicity (LD50) (mol/kg)	2.201	2.477	2.48	2.649	2.48	2.43
	Oral Rat Chronic Toxicity (LOAEL) (log mg/kg_bw/day)	1.947	4.981	5.231	3.183	5.647	4.25
	Hepatotoxicity (Yes/No)	No	No	No	No	No	No
	Skin Sensitization (Yes/No)	No	No	No	No	No	No
	***T. Pyriformis* toxicity (log ug/L)**	0.332	0.285	0.285	0.285	0.285	0.285
	Minnow toxicity (log mM)	2.585	-0.411	0.61	-1.524	4.348	0.276

Toxicity prediction

The toxicity predictions were performed to assess the safety profiles of various ligands using multiple toxicity tests, from the stoptox tool. The results indicate that all ligands, including L-1 the reference compound, L-11, L-5, L-17, L-15, and L-3, are

categorized as non-toxic for acute inhalation and oral exposure, suggesting minimal risk when these compounds are inhaled or ingested as mentioned in Table 4. However, there are significant concerns regarding acute dermal toxicity, as most ligands were found to be toxic upon skin contact, which could lead to adverse effects. For eye irritation and corrosion, all ligands except L-11 are deemed toxic, meaning they can cause irritation or damage to the eyes. In terms of skin sensitization, all ligands are identified as sensitizers, capable of inducing allergic reactions upon skin exposure. While most ligands are negative for skin irritation and corrosion, L-15 stands out with a positive result, indicating the potential for significant skin irritation or damage. In conclusion, L-11 stands out as the safest option among the ligands, exhibiting non-toxicity when inhaled, ingested, for eye irritation and corrosion while presenting lower risks compared to the others.

Table-4: Toxicity Parameters of the Selected Compounds by StopTox.

Ligands	Acute Inhalation Toxicity	Acute Oral Toxicity	Acute Dermal Toxicity	Eye Irritation and Corrosion	Skin Sensitization	Skin Irritation and Corrosion
L-1	Non-toxic	Non-toxic	Toxic	Toxic	Sensitizer	Negative
L-11	Non-toxic	Non-toxic	Toxic	Non-toxic	Sensitizer	Negative
L-5	Non-toxic	Non-toxic	Toxic	Toxic	Sensitizer	Negative
L-17	Non-toxic	Non-toxic	Toxic	Toxic	Sensitizer	Negative
L-15	Non-toxic	Non-toxic	Toxic	Toxic	Sensitizer	Positive
L-3	Non-toxic	Non-toxic	Toxic	Toxic	Sensitizer	Negative

Bioactivity Evaluation

The bioactivity prediction, using the Swiss Target Prediction tool, revealed that majority of the compounds were primarily predicted to target a range of protein types. These proteins include Family A G protein-coupled receptors, kinases, and oxidoreductases, which play crucial roles in numerous cellular processes. This is illustrated in Figure 7, where it is evident that many compounds have a strong affinity for these protein classes. This suggested that the compounds might have significant effects on pathways regulated by these proteins. Notably, Ellagic acid (L-1), the reference compound, showed a predominant interaction with Family A GPCRs (60%), alongside enzymes (20%) and kinases (6.7%). L-11 showed the most balanced interaction profile, with significant predicted interactions across multiple target classes, including Family A G protein-coupled receptors (33.3%), enzymes (20%), and kinases, suggesting broad biological activity. L-5 also demonstrated a diverse range of interactions, engaging nuclear receptors and enzymes, making it suitable for targeting specific signaling pathways. In contrast, L-17 exhibited a more targeted profile, with nearly half of its interactions (46.7%) aimed at Family A G protein-coupled receptors. This specificity could be advantageous if receptor modulation is the primary goal; however, it may not offer the broader applicability seen with L-11 or L-5. In summary, L-11 offers the best balance due to its interactions with a variety of biologically relevant targets, while L-17 might be the most effective if G protein-coupled receptor targeting is prioritized. The broad target profiles suggested these compounds may have diverse biological activities, potentially influencing multiple physiological processes and offering various therapeutic applications.

https://doi.org/10.35495/ajab.2024.248

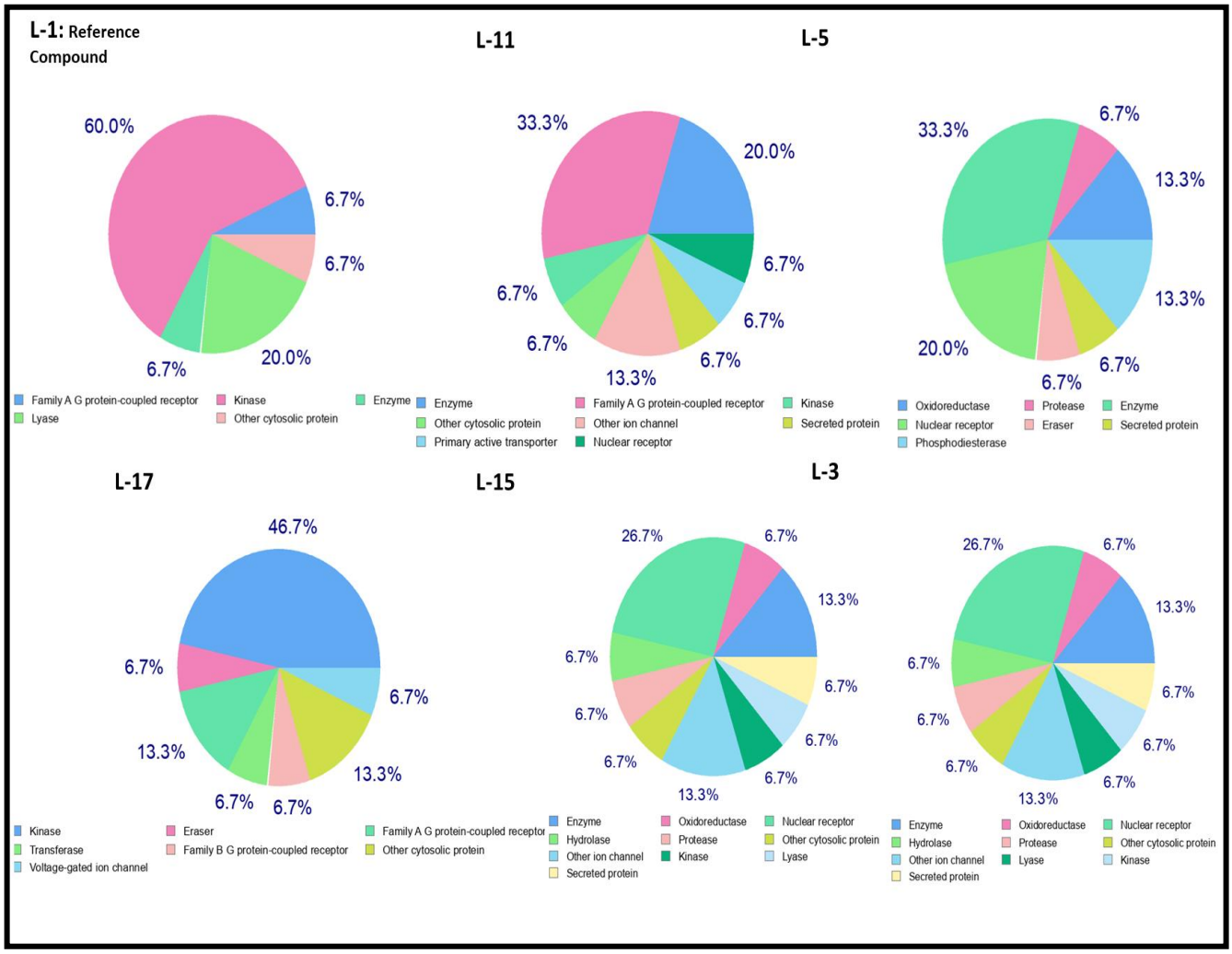

Figure-7: Swiss Target Prediction Analysis of the Top Compounds

DFT analysis

The selection of three ligands—L-1 (Reference Compound: EA), L-11, and L-5—was based on comprehensive ADMET profiling, which encompassed evaluations of bioavailability, pharmacokinetics, toxicity predictions, and bioactivity properties, as well as their binding affinities with the target Q55P57 protein. The DFT analysis in Table 5 compares the electronic properties of the three ligands against protein Q55P57.

L-11, with the highest dipole moment (12.0975 Debye), demonstrated enhanced polarity, suggesting stronger intermolecular interactions with the target protein. A higher dipole suggested stronger intermolecular interactions, such as hydrogen bonding or electrostatic forces, which can contribute to stable and specific binding of target protein. These interactions contribute can contribute to the more stable binding with protein, enhancing its affinity of ligand for the binding site. In this case, L-11 has the highest dipole moment, and also showed the highest docking score (-13.2kcal/mol), suggesting its enhanced polarity, contributing to its stronger binding affinity compared to other compounds. Its Highest Occupied Molecular Orbital (HOMO) energy (-0.14819eV) and Lowest Unoccupied Molecular Orbital (LUMO) energy (-0.04887eV) values indicated a small energy gap (ΔEGap = 2.7026 eV) compared to L-1 and L-5, both of which have significantly larger energy gaps. A smaller energy gap is associated with higher chemical reactivity, as it implies the molecule can easily participate in electron

transfer or other chemical interactions with the target protein. A smaller energy gap enhances the ability of the ligand to interact with the target, contributing to stronger binding. Despite these reactive tendencies, L-11 exhibited low electronegativity and electrophilicity, indicating a weaker ability to accept electrons. Additionally, L-11 has a higher softness (20.1369 eV^{-1}), making it more chemically flexible in terms of interactions. However, L-1 is relatively more stable due to the larger energy gap (-12.06581 eV) and less softness in comparison to L-2, and high polarity was shown by higher first electron affinity and electrophilicity values. L-5 is slightly above these two and hence has moderate reactivity and lower ionization potential to act like an electron donor. Overall, L-11 is the most reactive of the three ligands, characterized by its high dipole moment, small energy gap, and elevated softness, which indicated a strong tendency to interact with its environment.

Table 5: DFT analysis parameters of the top hit ligands

Ligand			
Parameters for DFT analysis	**L-1 (Reference Compound)**	**L-11**	**L-5**
Dipole moment (Debye	3.8253	12.0975	4.3267
HOMO(eV)	-0.21729	-0.14819	-0.13304
LUMO(eV)	-0.6607	-0.04887	-0.5748
Energy Gap (ΔE_{Gap}	-12.06581	2.7026	-12.0209
Ionization Potential (eV)	0.21729	0.14819	0.13304
Electron affinity (eV)	0.6607	0.04887	0.5748
Electronegativity χ (eV)	0.43899	0.09853	0.35392
Electrochemical potential μ (eV)	-0.43899	-0.09853	-0.35392
Hardness η (eV)	-0.2217	0.04966	-0.22088
Softness S (eV)	-4.5105	20.1369	-4.52734
Electrophilicity ω (eV)	0.096	0.00485	0.0626

The optimized structures, Frontier Molecular Orbitals (FMOs), and MEP maps of the top three ligands (L-1, L-11, L-5) docked to protein Q55P57, with L-1 as the reference compound are detailed in Figure 8. L-11, which shows a lower HOMO-LUMO energy gap indicates higher reactivity compared to L-1, making it the best candidate. In MEP maps, the charge distribution across the molecule from red (electron-rich areas) through blue (electron-deficient areas) is depicted, with L-11 showing distinct interaction regions that enhance binding affinity. Overall, L-11 emerged as the most promising ligand for interaction with the target protein due to its electronic properties and docking performance, providing a better understanding of its reactivity and potential as an inhibitor through electronic interactions with enzymes like laccase.

https://doi.org/10.35495/ajab.2024.248

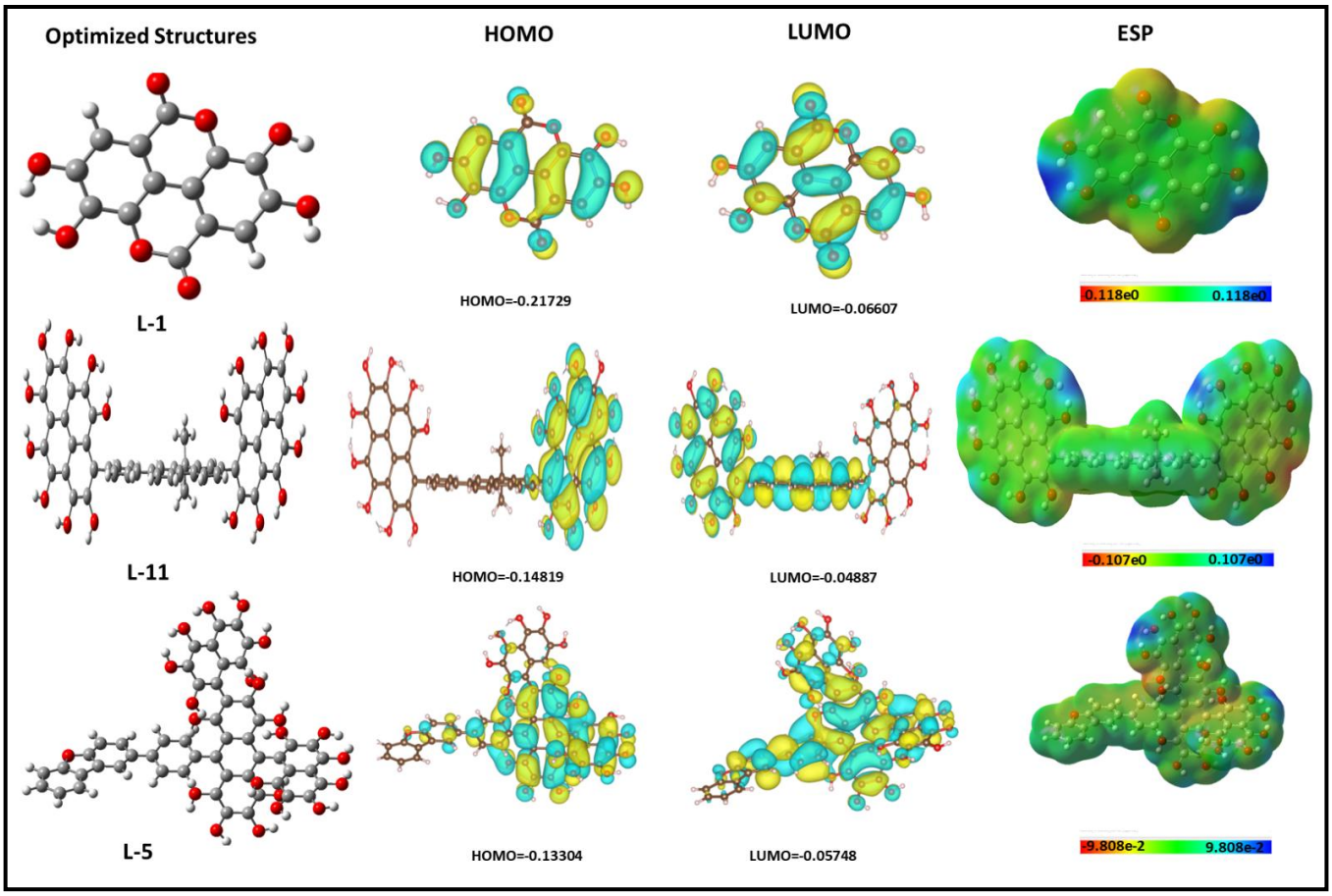

Figure-8: Optimized structural geometry showing FMO and MEP of the compounds L-1, L-11 and L-5.

Discussion

C. neoformans, ranked as a "critical" fungal pathogen by the WHO due to its antifungal resistance, limited therapeutic options, and high death rate, causes life-threatening cryptococcosis in immunocompromised hosts. The disease usually manifests as meningoencephalitis and is common in patients with HIV infection, organ transplant recipients, and patients receiving long-term immunosuppressive therapy. The clinical outcome depends on the interaction between the pathogen and the host immune system. In numerous developing countries, the availability of diagnostic services and treatment is restricted, while the rise of antifungal-resistant strains remains poorly understood (Chen et al., 2023; Zhao et al., 2023). The current study focuses on identifying and evaluating potential laccase inhibitors against *C. neoformans*. Using a combination of PBVS, molecular docking, ADMET profiling, bioactivity, and DFT analysis, we aimed to discover compounds with strong binding affinities and favorable drug-like properties, demonstrating high potential for therapeutic development against *C. neoformans* infections.

The validation of the Q55P57 protein structure confirmed its high stereochemical quality, making it suitable for computational analyses. The ERRAT analysis demonstrated a high-quality structure for laccase protein with an overall quality factor of 88.6%. The Ramachandran plot evaluation indicated that 86.5% of residues were located in the preferred regions, minimizing concerns about structural anomalies affecting protein-ligand interactions. This is consistent with another study showing 89.74% of residues in favored conformations and 3.17% as outliers (Azam et al., 2022). Another study also validated the experimental laccase structures revealed 99–100% of residues in the core and additional allowed regions (Mehra et al., 2018). These findings validated the Q55P57 model's reliability for exploring its functional interactions in *C. neoformans*, providing

a solid foundation for studying potential inhibitors and conducting further functional analyses.

Pharmacophore-based virtual screening was crucial in identifying potential inhibitors that align with the known characteristics of EA, a well-studied laccase inhibitor (Azam et al., 2022). By selecting the top 19 ligands with high similarity to the reference compound EA, this method effectively narrowed down candidates with favorable binding profiles for further docking analysis.

Molecular docking analysis of 19 compounds against the Q55P57 protein from the LAC1 enzyme of *C. neoformans* identified L-11 as the most promising candidate, with a docking score of -13.2 kcal/mol. L-11 effectively positioned itself within the active site, forming hydrogen bonds with residues such as H154, S166, T297, and D394, as well as hydrophobic contacts with L396 and F454. These residues are critical in fungal laccase activity as they may contribute to substrate binding and catalysis, indicating its potential as a leading laccase inhibitor for treating *C. neoformans* infections. These interactions are important because specific active site residues play crucial roles in the enzyme's function (Chitty et al., 2017). Several antifungal compounds, such as fluconazole, achieve effectiveness by binding more tightly to the active site of the fungal protein, despite minimal differences from its human counterpart (Ghannoum and Rice, 1999). Research has previously demonstrated the effectiveness of N-(butylcarbamothioyl) benzaminde (BTU-01), a synthetic compound, in combating *C. neoformans* through antifungal properties. Analysis using molecular docking showed that BTU-01 interacts strongly with crucial amino acid residues in the active site of urease *C. ensiformis*, which is a significant virulence factor in *Cryptococcus spp*. These findings suggested that BTU-01 could serve as a potential inhibitor of this enzyme (Andriani et al., 2023). Another study used molecular docking to evaluate hydrazide-hydrazone derivatives as laccase inhibitors. Docking results aligned with experimental data, highlighting their potential as antifungal agents (Maniak et al., 2021). These studies underscore the significance of molecular docking in identifying potent inhibitors and suggested that compounds with strong binding affinities to critical targets can aid in developing effective antifungal therapies.

Pharmacokinetic evaluation of L-11 showed promising properties, including moderate solubility and good Caco2 permeability for effective oral bioavailability (Pires et al., 2015)**.** Its higher volume of distribution and fraction unbound indicate robust tissue distribution, although moderate blood-brain barrier permeability may limit neuropharmacological applications. As a CYP3A4 substrate, L-11 carries potential drug-drug interaction risks, but its favorable toxicity profile and moderate maximum tolerated dose support its therapeutic potential against *C. neoformans*. Caution is advised due to possible hERG II inhibition, which could lead to cardiac side effects. Structural modifications such as reducing lipophilicity, decreasing alkalinity, introducing hydroxyl groups, adding acidic fragments, or imposing conformational constraints, can be used to mitigate the risk of hERG II inhibition in drug development, which could result in cardiac arrest (Guth and Rast, 2010; Garrido et al., 2020). Overall, L-11 is a strong candidate for development against fungal infections. Previous studies also emphasized that ADMET profiling aids in developing safer treatment regimens for both systemic and localized topical applications like the N-phenylbenzamide derivatives for antifungal infections (Sulistyowaty et al., 2023).

Toxicity predictions further refined the candidate pool, revealing that while all compounds were non-toxic via oral and inhalation exposure, ligands like L-15 raised concerns about skin sensitization and eye irritation, necessitating caution in drug development. To address these concerns, future studies could implement alternative in vitro assays to assess and mitigate these risks. For example, reconstructed human epidermis models can be used to assess the potential for skin irritation, and ocular models can be used to assess eye irritation, thereby reducing the need for animal testing and increasing human relevance (Vinardell and Mitjans, 2008). An oral combination of fluconazole and flucytosine shows a comparable infection clearance rate to amphotericin B and higher survival rates than fluconazole alone, emphasizing the oral route's effectiveness (Molloy et al., 2018)**.** Analysis of bioactivity Swiss Target Prediction showed that L-11 is a more promising candidate for therapeutic development against laccase enzymes in *C. neoformans* infections because it has a wider target profile with a range of biologically relevant targets.

Further analysis of L-11 using DFT stabilized its position as the top ligand, because its electronic properties were reported (Peverati and Truhlar, 2014). It is a highly polar ligand with a low energy gap, and high ionization potential, making it very reactive and

flexible toward the target enzyme. Such electronic properties give a molecular-level explanation for its better performance in docking studies. The final visualizations of the FMO and MEP maps provided crucial insights into charge distribution across these ligands, thereby reiterating that L-11 has the most favorable interaction profile with Q55P57.In a study, DFT studies showed that the antifungal effectiveness of the synthetic chalcones and pyrazolines against *C. neoformans* is primarily determined by their electrophilic nature. Chalcones with electron-withdrawing substituents exhibited greater electrophilic character, correlating with enhanced antifungal efficacy, highlighting the importance of electronic effects in developing effective antifungal agents (Illicachi et al., 2017). These findings collectively suggest that L-11 is not only a strong candidate based on docking but also exhibits desirable physicochemical and bioactive properties, making it a prime focus for further experimental validation against *C. neoformans* infections.

This study has, however, shown promising results but still has certain limitations. The analyses depended solely on in-silico approaches. These, though robust in their own sense, require some form of experimental validation to confirm the efficacy and safety of L-11 against *C. neoformans*. Future studies should focus on the optimization of L-11's structure toward increased selectivity and safety for antifungal activity and also its pharmacokinetic properties through further testing in-vitro and in-vivo. Its preclinical studies on its efficacy in animal models of cryptococcosis should also be included to establish the potential for its clinical development. These steps would bridge the gap between the predictions from computational means and practical applications that would permit L-11 to advance as a novel antifungal agent.

Conclusion

In conclusion, this study successfully identified L-11(8-[4-[9,9-Dimethyl-7-(2,3,4,5,6,7,8,9,10-nonahydroxypyren-1-yl)fluoren-2-yl]phenyl]pyrene-1,2,3,4,5,6,7,9,10-nonol) as a promising LAC1 inhibitor against *C. neoformans*. The integration of PBVS, molecular docking, and DFT revealed that L-11 exhibits strong binding affinity and desirable ADMET characteristics, making it a promising candidate for therapeutic research and development. Given its non-toxic profile and broad target interactions, further experimental validation and optimization of L-11 could pave the way for new antifungal strategies, particularly for immunocompromised individuals at risk of severe cryptococcal infections. Future work should focus on preclinical studies to assess in vivo efficacy and safety, followed by clinical trials to validate its therapeutic potential. This study highlighted the potential of computational methods in identifying novel antifungal agents, offering significant prospects for the development of targeted therapies against opportunistic pathogens like *C. neoformans*.

Acknowledgments

This research was supported by the Deanship of Graduate Studies and Scientific Research at Jouf University through the Fast-Track Research Funding Program. Heartfelt thanks are extended to all collaborators and team members for their invaluable contributions and support.

Disclaimer: None

Conflict of Interest: None

Source of Funding: This research wass funded by the Deanship of Graduate Studies and Scientific Research at Jouf University through the Fast-Track Research Funding Program.

Contribution of Authors

SY and HS: Wrote the initial manuscript.
MUK, YA & AEA: Performed the *In silico* analysis.
BBZM & KA: Drafted the figures and tables.
MA & HE: Critically reviewed and revised the manuscript and supervised the project.

All authors have read and agreed to the published version of the manuscript.

References

Andriani GM, Spoladori LFdA, Fabris M, Camargo PG, Pereira PML, Santos JP, Bartolomeu-Gonçalves G, Alonso L, Lancheros CAC, Alonso A, Nakamura CV, Macedo FJ, Pinge-Filho P, Yamauchi LM, Bispo MdLF, Tavares ER and Yamada-Ogatta SF, 2023. Synergistic antifungal interaction of N-(butylcarbamothioyl) benzamide and amphotericin B against Cryptococcus neoformans. Front. Microbiol. 14: 1040671. https://doi.org/10.3389/fmicb.2023.1040671.

Ayaz M, Ullah FSA, Ullah FOM, Ahmed J and Devkota HP, 2019. Synergistic interactions of phytochemicals with antimicrobial agents: Potential strategy to counteract drug resistance. Chem. Biol. Interact. 308: 294–303. https://doi.org/10.1016/j.cbi.2019.05.050.

Azam F, Khan MA, Khan A, Ahmad S, Zofair SFF and Younus H, 2022. In silico and in vitro studies on the inhibition of laccase activity by Ellagic acid: Implications in drug designing for the treatment of Cryptococcal infections. Int. J. Biol. Macromol. 209: 642–654. https://doi.org/10.1016/j.ijbiomac.2022.04.060.

Bastos RW, Rossato L, Goldman GH and Santos DA, 2021. Fungicide effects on human fungal pathogens: cross-resistance to medical drugs and beyond. PLoS Pathog. 17(12): 1010073. https://doi.org/10.1371/journal.ppat.1010073.

Borba JVB, Alves VM, Braga RC, Korn DR, Overdahl K, Silva AC, Hall SUS, Overdahl E, Kleinstreuer N, Strickland J, Allen D, Andrade CH, Muratov EN and Tropsha A, 2022. STopTox: An in silico alternative to animal testing for acute systemic and topical toxicity. Environ. Health Perspect. 130(2): 27012. https://doi.org/10.1289/EHP9341.

Cao Y, Song L, Miao Z, Hu Y, Tian L and Jiang T, 2011. Improved side-chain modeling by coupling clash-detection guided iterative search with rotamer relaxation. Bioinformatics. 27(6): 785–790. https://doi.org/10.1093/bioinformatics/btr009

Chen J, Shao J, Dai M, Fang W and Yang YL, 2023. Adaptive immunology of Cryptococcus neoformans infections-an update. Front. Immunol. 14: 1174967. https://doi.org/10.3389/fimmu.2023.1174967

Chitty JL, Blake KL, Blundell RD, Koh YQAE, Thompson M, Robertson AAB, Butler MS, Cooper MA, Kappler U, Williams SJ, Kobe B and Fraser JA, 2017. Cryptococcus neoformans ADS lyase is an enzyme essential for virulence whose crystal structure reveals features exploitable in antifungal drug design. J. Biol. Chem. 292(28): 11829–11839. https://doi.org/10.1074/jbc.M117.787994

Colovos C and Yeates TO, 1993. Verification of protein structures: patterns of nonbonded atomic interactions. Protein Sci. 2(9): 1511–1519.https://doi.org/10.1002/pro.5560020916

Daina A and Zoete V, 2024. Testing the predictive power of reverse screening to infer drug targets, with the help of machine learning. Commun. Chem. 7(1):105. https://doi.org/10.1038/s42004-024-01179-2

Datta A, Yadav V, Ghosh A, Choi J, Bhattacharyya D, Kar RK, Ilyas H, Dutta A, An E, Mukhopadhyay J, Lee D, Sanyal K, Ramamoorthy A and Bhunia A, 2016. Mode of action of a designed antimicrobial peptide: high potency against Cryptococcus neoformans. Biophys J. 111(8): 1724–1737. https://doi.org/10.1016/j.bpj.2016.08.032

Eberhardt J, Santos-Martins D, Tillack AF and Forli S, 2021. AutoDock Vina 1.2.0: New docking methods, expanded force field, and python bindings. JCIM. 61(8): 3891–3898. https://doi.org/10.1021/acs.jcim.1c00203

Fisher MC, Alastruey-Izquierdo A, Berman J, Bicanic T, Bignell EM, Bowyer P, Bromley M, Brüggemann R, Garber G, Cornely OA, Gurr SJ, Harrison TS, Kuijper E, Rhodes J, Sheppard DC, Warris A, White PL, Xu J, Zwaan B and Verweij PE, 2022. Tackling the emerging threat of antifungal resistance to human health. Nat. Rev. Microbiol. 20(9): 557–571. https://doi.org/10.1038/s41579-022-00720-1

Garrido A, Lepailleur A, Mignani SM, Dallemagne P and Rochais C, 2020. hERG toxicity assessment: Useful guidelines for drug design. Eur. J. Med. Chem. 195: 112290. https://doi.org/10.1016/j.ejmech.2020.112290

Ghannoum MA and Rice LB, 1999. Antifungal agents: mode of action, mechanisms of resistance, and correlation of these mechanisms with bacterial resistance. Clin. Microbiol. Rev. 12(4): 501–517. https://doi.org/10.1128/CMR.12.4.501.

Guth BD and Rast G, 2010. Dealing with hERG liabilities early: diverse approaches to an important goal in drug development. Br. J. Pharmacol. 159(1): 22–24. https://doi.org/10.1111/j.1476-5381.2009.00265.x.

Gutierrez-Gongora D and Geddes-McAlister J, 2022. Peptidases: promising antifungal targets of the human fungal pathogen, Cryptococcus neoformans. Facets. 7(1): 319–342. http://dx.doi.org/10.1139/facets-2021-0157.

Huang YS, Liu CE, Lin SP, Lee CH, Yang CJ, Lin CY, Tang HJ, Lee YC, Lin YC, Lee YT, Sun HY and Hung CC, 2019. Echinocandins as alternative treatment for HIV-infected patients with Pneumocystis pneumonia. AIDS. 33(8): 1345–1351. https://doi.org/10.1097/QAD.0000000000002207

Illicachi LA, Montalvo-Acosta JJ, Insuasty A, Quiroga J, Abonia R, Sortino M, Zacchino S and Insuasty B, 2017. Synthesis and DFT calculations of novel vanillin-chalcones and their 3-Aryl-5-(4-(2-(dimethylamino)-ethoxy)-3-methoxyphenyl)-4,5-dihydro-1H-pyrazole-1-carbaldehyde derivatives as antifungal agents. Molecules. 22(9): 1476. https://doi.org/10.3390/molecules22091476

Islam S, Hussain EA, Shujaat S, Khan MU, Ali Q, Malook SU and Ali D, 2024. Antibacterial potential of Propolis: molecular docking, simulation and toxicity analysis. AMB Express. 14(1): 81. https://doi.org/10.1186/s13568-024-01741-0.

Khan MA, Khan A, Azam M, Allemailem KS, Alrumaihi F, Almatroudi A, A Alhumaydhi F, Azam F, Khan SH, Zofair SFF, Ahmad S and Younus H, 2021. Liposomal ellagic acid alleviates cyclophosphamide-induced toxicity and eliminates the systemic Cryptococcus neoformans infection in leukopenic mice. Pharmaceutics. 13(6): 882. https://doi.org/10.3390/pharmaceutics13060882.

Khan MF, Ali A, Rehman HM, Noor Khan S, Hammad HM, Waseem M, Wu Y, Clark TG and Jabbar A, 2024. Exploring optimal drug targets through subtractive proteomics analysis and pangenomic insights for tailored drug design in tuberculosis. Sci. Rep. 14(1): 10904. https://doi.org/10.1038/s41598-024-61752-6.

Khan MU, Sakhawat A, Rehman R, Wali AH, Ghani MU, Akram A, Javed MA, Ali Q, Yu-Ming Z and Ali D, 2024. Identification of novel natural compounds against CFTR p. Gly628Arg pathogenic variant. AMB Express. 14(1): 99. https://doi.org/10.1186/s13568-024-01762-9.

Langeveld WT, Veldhuizen EJA and Burt SA, 2014. Synergy between essential oil components and antibiotics: a review. Crit. Rev. Microbiol. 40(1): 76–94. https://doi.org/10.3109/1040841X.2013.763219.

Laniado-Laborín R and Cabrales-Vargas MN, 2009. Amphotericin B: side effects and toxicity Revista iberoamericana de micologia. 26(4): 223–227. https://doi.org/10.1016/j.riam.2009.06.003.

Laskowski RA, Rullmannn JA, MacArthur MW, Kaptein R and Thornton JM, 1996. AQUA and PROCHECK-NMR: programs for checking the quality of protein structures solved by NMR. J. Biomol. NMR. 8(4): 477–486. https://doi.org/10.1007/BF00228148.

Liu Y, Yang X, Gan J, Chen S, Xiao ZX and Cao Y, 2022. CB-Dock2: improved protein-ligand blind docking by integrating cavity detection, docking and homologous template fitting. Nucleic Acids Res. 50(W1): W159–W164. https://doi.org/10.1093/nar/gkac394.

Maniak H, Talma M and Giurg M, 2021. Inhibitory potential of new phenolic hydrazide-hydrazones with a decoy substrate fragment towards laccase from a phytopathogenic fungus: SAR and molecular docking studies. Int. J. Mol. Sci. 22(22): 12307. https://doi.org/10.3390/ijms222212307.

Mehra R, Muschiol J, Meyer AS and Kepp KP, 2018. A structural-chemical explanation of fungal laccase activity. Sci. Rep. 8(1): 17285. https://doi.org/10.1038/s41598-018-35633-8.

Molloy SF, Kanyama C, Heyderman RS, Loyse A, Kouanfack C, Chanda D, Mfinanga S, Temfack E, Lakhi S, Lesikari S, Chan AK, Stone N, Kalata N, Karunaharan N, Gaskell K, Peirse M, Ellis J, Chawinga C, Lontsi S, Ndong JG, Bright P, Lupiya D, Chen T, Bradley J, Adams J, van der Horst C, van Oosterhout JJ, Sini V, Mapoure YN, Mwaba P, Bicanic T, Lalloo DG, Wang D, Hosseinipour MC, Lortholary O, Jaffar S and Harrison TS, 2018. Antifungal combinations for treatment of cryptococcal meningitis in Africa. N. Engl. J. Med. 378(11): 1004–1017. https://doi.org/10.1056/NEJMoa1710922.

Moreira-Walsh B, Ragsdale A, Lam W, Upadhya R, Xu E, Lodge JK and Donlin MJ, 2022. Membrane integrity contributes to resistance of cryptococcus neoformans to the cell wall inhibitor caspofungin. mSphere. 7(4): e0013422. https://doi.org/10.1128/msphere.00134-22.

Mourad A and Perfect JR, 2018. The war on cryptococcosis: a review of the antifungal arsenal. Mem. Inst. Oswaldo Cruz. 113(7): e170391. https://doi.org/10.1590/0074-02760170391.

Norhayati EJ, Diyah NW, Tejo BA and Ahmed S, 2023. Chemoinformatics approach to design and develop vanillin analogs as COX-1 inhibitor. J. Public Health Afr. 14(Suppl 1): 2517. https://doi.org/10.4081/jphia.2023.2517.

World Health Organization (WHO), 2022. WHO fungal priority pathogens list to guide research, development and public health action. World Health Organization, Geneva, Switzerland.

Orio M, Pantazis DA and Neese F, 2009. Density functional theory. Photosynth. Res. 102(2–3): 443–453. https://doi.org/10.1007/s11120-009-9404-8.

Peverati R and Truhlar DG, 2014. Quest for a universal density functional: the accuracy of density functionals across a broad spectrum of databases in chemistry and physics. Philos. Trans. A Math. Phys. Eng. Sci. 372(2011): 20120476. https://doi.org/10.1098/rsta.2012.0476.

Pires DEV, Blundell TL and Ascher DB, 2015. pkCSM: predicting small-molecule pharmacokinetic and toxicity properties using graph-based signatures. J. Med. Chem. 58(9): 4066–4072. https://doi.org/10.1021/acs.jmedchem.5b00104.

Qadri H, Shah AH and Mir M, 2021. Novel strategies to combat the emerging drug resistance in human pathogenic microbes. Curr. Drug Targets. 22(12): 1424–1436. https://doi.org/10.2174/1389450121666201228123212.

Ríos JL, Giner RM, Marín M and Recio MC, 2018. A pharmacological update of ellagic acid. Planta Med. 84(15): 1068–1093. https://doi.org/10.1055/a-0633-9492.

Sakhawat A, Awan SJ, Khan MU, Shahid S, Maqbool T, Zubair HM, Manzoor H and Khan S, 2024. In silico and in vitro analyses to investigate the effects of vitamin C on VEGF protein. J. Taibah Univ. Med. Sci. 19(4): 775–789. https://doi.org/10.1016/j.jtumed.2024.06.008.

Sakhawat A, Khan MU, Rehman R, Khan S, Shan MA, Batool A, Javed MA and Ali Q, 2023. Natural compound targeting BDNF V66M variant: insights from in silico docking and molecular analysis. AMB Express. 13(1): 134. https://doi.org/10.1186/s13568-023-01640-w.

Sarkar S, Siddiqui AA, Mazumder S, De R, Saha SJ, Banerjee C, Iqbal MS, Adhikari S, Alam A, Roy S and Bandyopadhyay U, 2015. Ellagic Acid, a dietary polyphenol, inhibits tautomerase activity of human macrophage migration inhibitory factor and its pro-inflammatory responses in human peripheral blood mononuclear cells. J. Agric. Food Chem. 63(20): 4988–4998. https://doi.org/10.1021/acs.jafc.5b00921.

Singh S, Fatima Z and Hameed S, 2015. Predisposing factors endorsing Candida infections. Infez. Med. 23(3): 211–223.

Sulistyowaty MI, Putra GS, Budiati T, Indrianingsih AW, Anwari F, Kesuma D, Matsunami K and Yamauchi T, 2023. Synthesis, In Silico Study, Antibacterial and Antifungal Activities of N-phenylbenzamides. Int. J. Mol. Sci. 24(3): 2745. https://doi.org/10.3390/ijms24032745.

Sunseri J and Koes DR, 2016. Pharmit: interactive exploration of chemical space. Nucleic Acids Res. 44(W1): W442–W448.

Varadi M, Bertoni D, Magana P, Paramval U, Pidruchna I, Radhakrishnan M, Tsenkov M, Nair S, Mirdita M, Yeo J, Kovalevskiy O, Tunyasuvunakool K, Laydon A, Žídek A, Tomlinson H, Hariharan D, Abrahamson J, Green T, Jumper J, Birney E, Steinegger M, Hassabis D and Velankar S, 2024. AlphaFold Protein Structure Database in 2024: providing structure coverage for over 214 million protein sequences. Nucleic Acids Res. 52(D1): D368–D375. https://doi.org/10.1093/nar/gkad1011.

Vinardell MP and Mitjans M, 2008. Alternative methods for eye and skin irritation tests: an overview. J. Pharm. Sci. 97(1): 46–59. https://doi.org/10.1002/jps.21088.

Yang X, Liu Y, Gan J, Xiao ZX and Cao Y, 2022. FitDock: protein-ligand docking by template fitting. Brief. Bioinform. 23(3): bbac087. https://doi.org/10.1093/bib/bbac087.

Zhao Y, Ye L, Zhao F, Zhang L, Lu Z, Chu T, Wang S, Liu Z, Sun Y, Chen M, Liao G, Ding C, Xu Y, Liao W and Wang L, 2023. Cryptococcus neoformans, a global threat to human health. Infect. Dis. Poverty. 12(1): 20. https://doi.org/10.1186/s40249-023-01073-4.

Zhu X, Gibbons J, Garcia-Rivera J, Casadevall A and Williamson PR, 2001. Laccase of Cryptococcus neoformans is a cell wall-associated virulence factor. Infect. Immun. 69(9): 5589–5596. https://doi.org/10.1128/IAI.69.9.5589-5596.2001.